TECHNICAL MEMORANDUM

586

The RTTOV-9 upgrade for clear-sky radiance assimilation in the IFS

Niels Bormann, Deborah Salmond, Marco Matricardi, Alan Geer, Mats Hamrud

Research Department

March 2009

European Centre for Medium-Range Weather Forecasts
Europäisches Zentrum für mittelfristige Wettervorhersage
Centre européen pour les prévisions météorologiques à moyen terme

Series: ECMWF Technical Memoranda

A full list of ECMWF Publications can be found on our web site under:
http://www.ecmwf.int/publications/

Contact: library@ecmwf.int

European Centre for Medium-Range Weather Forecasts
Shinfield Park, Reading, RG2 9AX, England

Abstract

The memorandum describes the impact of the upgrade to RTTOV-9 on the assimilation of clear-sky radiances in the ECMWF system. The upgrade includes the use of the new linear-in-tau parameterisation of the source function, the inclusion of the effect of variable zenith angles with height, the use of the new internal interpolation provided by RTTOV-9, and an upgrade to the coefficient files used for RTTOV. The latter includes a move towards kCARTA-based coefficients for infrared sensors.

A detailed analysis of the components of the upgrade shows that the changes primarily alter bias characteristics of the assimilated radiances, prompting different responses of the air-mass dependent bias correction. One of the largest changes is due to the move to kCARTA-based RTTOV coefficients which leads to a significant reduction of the absolute size of the corrections for HIRS. After bias correction, most departure statistics for assimilated radiances are overall largely unaltered. Exceptions are reductions in the size of First Guess departures for lower tropospheric HIRS channels resulting from the kCARTA coefficients, and, for specific periods, reductions in the size of First Guess departures for some high-peaking IASI channels which benefit from improvements towards the model top, related to the use of the RTTOV internal interpolation. The use of the RTTOV internal interpolation successfully avoids spikes previously seen in gradients from the radiance data on model profiles.

The forecast impact of the upgrade is overall neutral. Mean temperature analyses close to the forecast model's top are considerably altered, as a result of an improved handling of temperature information near the forecast model's top.

1 Introduction

RTTOV is the fast radiative transfer model used at ECMWF and elsewhere for the assimilation of nadir microwave or infrared radiances (e.g., Saunders et al. 1999, Matricardi et al. 2004). It uses regression models to parameterise the effective layer optical depth for each channel, with regression coefficients derived from accurate line-by-line calculations for a representative sample of atmospheric profiles and viewing angles. The coefficients are derived for layers defined by fixed pressure levels. RTTOV models the contributions of the relevant atmospheric gases; some key atmospheric gases are allowed to vary (e.g., water vapour and ozone), whereas a fixed climatological profile is assumed for all others. RTTOV includes fast surface emissivity models over oceans, namely FASTEM (e.g., DeBlonde and English 2001) for the microwave and ISEM (Sherlock 1999) for the infrared. RTTOV can simulate clear-sky radiances, and additional codes are available to include either the effects of cloud emissions, or scattering effects in the microwave. The latter is known as RTTOV_SCATT and is being used at ECMWF for the assimilation of rain-affected microwave radiances (e.g., Geer et al. 2008). RTTOV is developed and maintained through the Numerical Weather Prediction (NWP) Satellite Application Facility (SAF), coordinated by the Met.Office, and ECMWF serves as beta-tester before general code releases.

RTTOV-9 is the latest version of the RTTOV package (e.g., Saunders et al. 2008). Improvements in RTTOV-9 include a new linear-in-tau parameterisation of the source function in the radiative transfer integration, the option of a variable zenith angle to account for the curvature of Earth, and the option to supply CO_2, N_2O, CO, and CH_4 as variable gases. It also allows the user to provide atmospheric profiles on any (reasonable) pressure levels instead of the fixed RTTOV pressure levels, and it employs a sophisticated interpolation to obtain the values on the internally used fixed pressure levels. This interpolation avoids spikes and missing levels in the gradients otherwise commonly encountered when using a linear interpolation (Rochon et al. 2007). Cloud calculations are now included in the main code (previously done by RTTOV_CLOUD), and they have been completely rewritten based on a multiple scattering parameterisation (Matricardi 2005). This feature is intended for use with infrared radiances, but the code could be extended for modelling cloud emissions in the microwave as well. An aerosol capability is included as well (Matricardi 2005), as is the optional simulation of reflected solar radiation. RTTOV_SCATT has been upgraded as well to make it compatible with the clear-sky RTTOV-9

changes.

This memorandum describes the upgrade of RTTOV used in ECMWF's Integrated Forecast System (IFS) from version 8 to version 9, as was introduced in cycle 35r2. We describe the performance of RTTOV-9 for clear-sky radiance assimilation, and focus on the aspects directly applicable to operational use. These include the linear-in-tau parameterisation, the variable zenith angle, and the use of the new interpolation within RTTOV. The cloud computations for infrared are used operationally in the post-processing for the satellite image simulations, but are not described here. The capability to model effects of other gases or aerosols is relevant for the GEMS project, but only water vapour and ozone are used as variable gases in the operational analysis. Other features of RTTOV-9 such as the modelling of solar reflection are left for future evaluations.

Also included in the upgrade discussed here is an update of the set of coefficient files describing the regressions for the layer optical depths. This update is independent of the implementation of RTTOV-9, but is combined in the current upgrade, as it also significantly affects the radiance computations.

The structure of the memorandum is as follows: We will first describe the new features and coefficient files to be used for RTTOV in the operational configuration of the IFS. We will then characterise the analysis impact of these new features and new coefficient files separately, to highlight their relative role in the analysis. Following this, we will summarise the analysis and forecast impact of the combined changes. A summary and conclusions are given in the last section.

2 RTTOV-9 upgrade in the IFS

The RTTOV-9 upgrade in the IFS consists of the following elements:

- Use of new RTTOV-9 features excluding the internal interpolation: Linear-in-tau parameterisation, variable zenith angle.
- Revision of the set of coefficient files used in the assimilation.
- Use of the internal RTTOV interpolation.

These will be described in more detail below. For further details on the methods or their implementation in RTTOV-9 see Saunders et al. (2008).

Another change specific to the IFS-version of RTTOV-8 affects the simulation of ocean surface emissivity in the microwave. The IFS-version of RTTOV-8 has a missing term in the permittivity calculations of FASTEM that was included in the general release of RTTOV-8, but not included in the IFS. Introduction of the term leads to a shift in the bias correction applied to SSMI and similar clear-sky radiances of typically 1-3 K (depending on channel), but otherwise negligible differences in the overall First Guess (FG) or analysis departures. For SSMI instruments, this means larger bias corrections, whereas for TMI the extra term leads to a reduction of bias corrections in absolute terms. In the remainder, the effect of the extra term is not included.

2.1 Linear-in-tau parameterisation, variable zenith angle

Previous versions of RTTOV have calculated the layer source function used in the radiative transfer integral from a simple average of the top and the bottom layer temperature. This is suboptimal for optically thick layers.

The new linear-in-tau parameterisation assumes that the layer temperature varies linearly with the optical depth between the top and the bottom values.

The variable zenith angle feature takes into account the curvature of the Earth, instead of the previous assumption of a constant zenith angle, appropriate for the plane-parallel atmosphere assumption. Note that effects due to refraction can also be included in RTTOV-9, but these are not studied here, as the effect is small for the nadir radiances assimilated in the ECMWF system.

2.2 New coefficient files

The set of coefficient files currently used at ECMWF has been compiled when RTTOV-8 was introduced in the IFS, and it was felt that the upgrade to the RTTOV-9 code should be accompanied with a move to coefficient files derived from more recent spectroscopy or improved training sets. The current set mostly employs RTTOV-7 regression models (Matricardi et al. 2001), derived from GENLN2 line-by-line calculations for the infrared (Edwards 1992), and calculations with the Liebe model in the microwave (Liebe 1989, Liebe et al. 1992). The exception are the radiative transfer coefficients for IASI which are based on kCARTA V1.11 computations (DeSouza-Machado et al. 1997, 1999), but also employ the RTTOV-7 regression model. All coefficient files are provided for 43 pressure levels.

The new set of coefficient files comprises the following updates:

- Use of kCARTA-based coefficients for all infrared sensors, derived from the ECMWF 60-level diverse profile dataset. These also employ the RTTOV-8 predictor model which parameterises line and continuum effects through separate regression models (Matricardi 2003), instead of a single combined one. The move to kCARTA coefficients was motivated by the finding that comparisons for IASI showed that kCARTA-based coefficients gave better results than GENLN2 ones (Collard 2008, pers. communication). This is a result of improved spectroscopy in kCARTA, in particular the inclusion of P/R-branch line mixing and the use of HITRAN2000 (instead of HITRAN96 used in the previous GENLN2-based coefficients).

- For infrared instruments with very broad spectral response functions (such as geostationary imagers) coefficients calculated from Planck-weighted transmittances are used. This aims to better incorporate the variation of the Planck function with wavenumber.

- For microwave instruments, the use of the RTTOV-7 predictor model is retained, following a recommendation by Roger Saunders (2008, pers. communication). For AMSU-B/MHS, coefficients from a more recent training dataset are used. FASTEM-3 is used for the surface emissivity instead of FASTEM-2 where possible; for SSMI, SSMIS, and TMI the azimuth angle required for FASTEM-3 is currently not provided with the observations and therefore FASTEM-2 is used.

- For AMSU-A, the only update is the use of FASTEM-3 - otherwise the coefficients that exclude the Zeeman effect in the line-by-line calculations are retained (Kobayashi et al. 2007).

For AIRS, the old GENLN2 coefficients included channel-specific γ-coefficients used to scale the optical depths in the radiative transfer integral (Watts and McNally 2004). These were derived to reduce biases between simulated and observed AIRS radiances, and they are used in combination with the general variational bias correction. For the updated coefficient file, no new γ-coefficients have been calculated (i.e., all γs are equal to one).

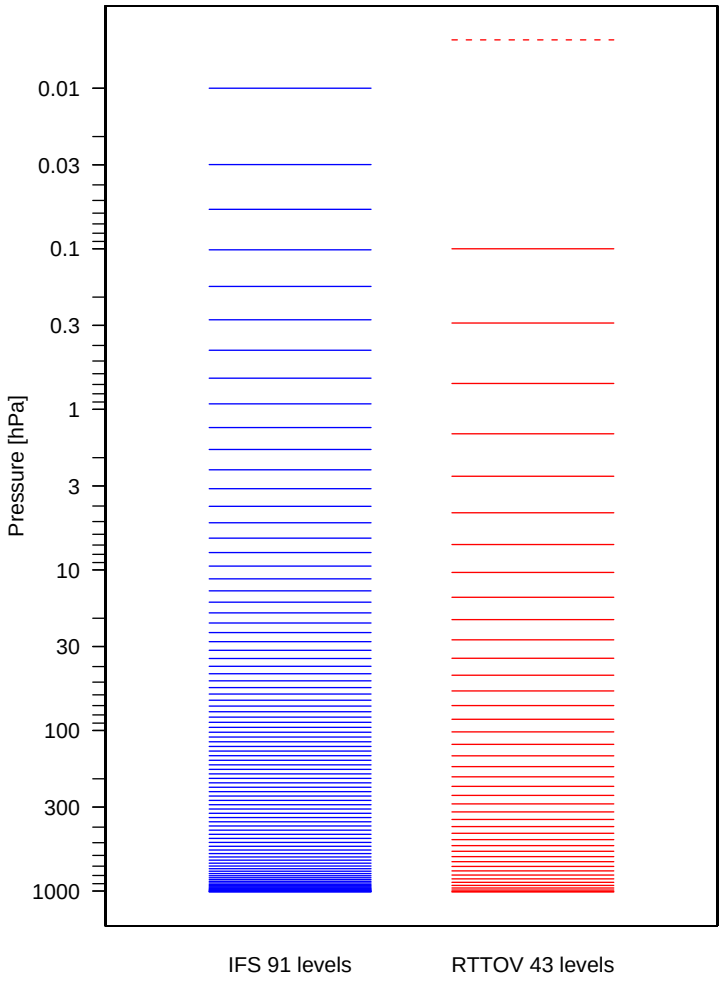

Figure 1: IFS 91 model levels for a standard surface pressure (blue) and the 43 RTTOV fixed pressure levels (red). The red dashed line indicates the top of the atmosphere assumed in the line-by-line calculations used to train RTTOV.

All coefficients again use 43 pressure levels shown in Fig. 1 to describe the regressions for the optical depths. Recently, new coefficient files based on LBLRTM calculations have become available for infrared sensors (e.g., Matricardi and McNally 2008), and they should be studied further for assimilation puposes at a later stage.

2.3 RTTOV interpolation

An interesting innovation of RTTOV-9 is the option to provide atmospheric input profiles on any set of (reasonable) pressure levels ("user levels"). In older versions, the user was required to provide profiles already interpolated to the fixed pressure levels used in RTTOV for the optical depth parameterisation. At ECMWF, the required interpolation from model to RTTOV levels has been done using a linear interpolation (see Fig. 1 for a comparison of the 91 IFS levels and the 43 RTTOV levels). The effect of this was that model-level gradients obtained from radiance calculations exhibited spikes and "blind" levels particularly in areas where the RTTOV vertical resolution is much poorer than that of the IFS (e.g., upper stratosphere), as some model levels contributed little or not at all to the radiance calculations.

The new RTTOV-internal interpolation is designed to avoid spikes or "blind" levels in gradients or Jacobians (Rochon et al. 2007). This is achieved by calculating the interpolated value as a weighted integral over all user levels that fall within the range spanned by the RTTOV levels neighbouring the RTTOV level to be interpolated to. The weighting is triangular in the logarithm of pressure, with zero weights at the neighbouring RTTOV levels and maximum weight at the RTTOV level to interpolate to. The approach ensures that all user levels are used in the RTTOV computations. Use of the RTTOV interpolation will alter somewhat the interpretation of the profile information compared to a linear interpolation due to the implicit smoothing of the profile. For instance, in areas with high curvature (e.g., tropopause, stratopause), the new interpolation will be systematically colder or warmer than the linear interpolation, depending on the orientation of the curvature.

With the implementation of RTTOV-9 in the IFS, the option has been introduced to provide atmospheric input profiles to RTTOV directly on the IFS model levels. Due to the way the interpolation option is implemented in RTTOV, this option changes substantially the role of the interpolation beyond merely replacing one method with another. For the current practice of using the IFS interpolation, all input to RTTOV is provided on RTTOV-levels, and optical depth calculations as well as the radiative transfer integration inside RTTOV are performed on these RTTOV-levels. In contrast, when the input is provided on model levels in RTTOV-9, profile values are interpolated to RTTOV-levels for the optical depth calculations only. Following the optical depth calculations, the total optical depth is interpolated to the model levels, using the same interpolation method as for the atmospheric variables, and the radiative transfer integration is subsequently performed on the model levels. This has the advantage that the full IFS temperature profile is used to specify the source function in the radiative transfer integration. However, it also adds an additional computational cost to the radiative transfer computations beyond introducing a more computationally expensive interpolation, as for the IFS 91 level model the radiative transfer integration is then performed on 91 model levels, rather than 43 RTTOV levels.

Performing the radiative transfer integration on model levels has another important implication for the IFS near the model top. For historical reasons, RTTOV assumes an isothermal layer between the top of the atmosphere (assumed to be at 0.005 hPa) and the next provided level, with the temperature specified by the latter level. When the interpolation is done outside RTTOV, the isothermal layer extends from 0.1 hPa to 0.005 hPa for 43-level coefficient files (Fig. 1), and any information available in the IFS on the temperature structure above 0.1 hPa is ignored. Assuming isothermal conditions for such a broad layer in the mesosphere is of course a very poor assumption. In contrast, if the internal RTTOV interpolation is employed within the 91-level IFS setup, information available in the IFS on the temperature structure above 0.1 hPa is used in the radiative transfer integration and the isothermal layer extends only from 0.01 hPa (the top of the IFS model) to 0.005 hPa. This will obviously have an effect on radiance simulations for channels with significant contributions from near the RTTOV top of the atmosphere[1].

[1]Note in this context that in RTTOV-9.2 the extrapolation of the optical depths towards the top user level is incorrect when the internal interpolation is used, as a constant optical depth is assumed above 0.1 hPa. This bug has been fixed in the IFS and does not apply to the statistics shown here. Another bug related to the isothermal assumption is present in the predictor calculation for the optical depth parameterisation for the top layer in RTTOV, and this bug is also present in the statistics presented here. The handling of the top of the atmosphere will be corrected and improved in RTTOV-10.

3 Impact of the components of the upgrade on departures and analyses

3.1 Assimilation experiments

We will now characterise the individual effects of the three groups of features introduced above on FG departures, bias corrections, and mean analyses in the assimilation. This will be done on the basis of lower-resolution experiments with the IFS, with a model and analysis resolution of T159 (≈125 km), and 91 levels in the vertical up to 0.01 hPa. The experiments cover the period September 2007, and, due to technical reasons, they exclude the assimilation of rainy radiances. The following experiments were performed[2]:

Control: RTTOV-8 with the old coefficients.

RT9: Use RTTOV-9 with the linear-in-tau parameterisation and the variable zenith angle feature. Old coefficient files.

RT9NewCoef: As RT9, but with the new set of coefficient files.

RT9NewCoefInterpol: As RT9NewCoef, but also using the RTTOV-9 internal interpolation.

All experiments use variational bias correction (VarBC, e.g., Dee 2004). As the radiance simulations for the various configurations are expected to lead to different bias characteristics for some radiances, VarBC was cold-started with the mode of the First-Guess departures at the beginning of these experiments. This means all coefficients for the bias-correction models were initialised to zero at the beginning of each experiment, except the flat component which was set to the mode of the First Guess departures for the first cycle. Subsequently, the bias coefficients are allowed to evolve through the VarBC method as usual. The bias correction for most radiances uses four air-mass predictors (reflecting the 1000-300 hPa, 200-50 hPa, 50-5 hPa, and 10-1 hPa layer thicknesses). Exceptions are the geostationary water vapour radiances which use 1000-300 hPa and 200-50 hPa layer thicknesses and total column water vapour, and the microwave imagers which use surface temperature and wind speed, and total column water vapour as air-mass predictors. Except for the geostationary radiances, all radiances use a third or fourth order polynomial in the scan position to correct for scan biases. For AMSU-A channel 14, no bias correction is used, in order to anchor stratospheric temperatures. To allow the bias coefficients to spin up sufficiently, we will present results for the second half of the experiments only.

Bias correction is an integral part of the assimilation of radiances and therefore also plays an important role for the evaluation of the radiative transfer changes investigated in this memorandum. Changes in the radiative transfer will lead to different FG departures, which will lead to differences in the analyses or to differences in the bias correction, depending on the relative cost associated with the modification. Once the bias correction has spun up, the analysis increments will be primarily determined by FG departures after bias correction. Within the assimilation, it is therefore of particular importance to what extent modifications to the radiative transfer can reduce differences between observed and simulated radiances beyond what can be accounted for by a well-chosen bias correction.

While the RTTOV-9 changes affect all radiances assimilated at ECMWF, we will focus here on the ATOVS family of instruments, AIRS, and IASI. Other instruments (geostationary imagers, microwave imagers) tend to show similar changes in the characteristics, but not all of these will be mentioned.

[2] Note that these experiments are based on a pre-release version of RTTOV-9, but differences to the final RTTOV-9 have been found to be small.

3.2 Linear-in-tau parameterisation and use of variable zenith angle

We will now compare the experiments Control and RT9 to characterise the effect of using the linear-in-tau parameterisation and the variable zenith angle feature of RTTOV-9.

The most notable differences for assimilated radiances are some changes in the bias correction for some channels. For instance, stratospheric AMSU-A channels (10-13) exhibit a decrease in the mean bias correction of up to 0.2 K (Fig. 2). This is a reduction in absolute terms for most NOAA satellites, but an increase in absolute terms for METOP. The two satellite series show different bias characteristics, as different versions of the antenna pattern corrections are applied to the data. Smaller absolute bias corrections are usually seen as a positive sign, yet the uncertainty in, for instance, the antenna pattern correction or in FG biases in the stratosphere make it difficult to draw a firm conclusion. The change in the mean bias correction is accompanied with a slight reduction in the standard deviation of the bias correction for channels 12 and 13, suggesting that less spatial structure is required in the bias corrections when the new RTTOV-9 features are used.

The change in the AMSU-A bias corrections is largely a response of assimilating channel 14 without a bias correction, together with altering the bias in the forward model through the new RTTOV-9 features. Because channel 14 is assimilated without a bias correction and the bias in the forward model has changed, the stratospheric temperature analysis is forced to respond to this different bias. This largely explains the differences in the zonal mean temperature analysis displayed in Fig. 3. For other AMSU-A channels, the bias correction then responds to the different bias characteristics of the model fields as well as the different bias characteristics of the forward model. The warming at around 5-10 hPa shown in the zonal mean is also evident in departure statistics for radiosonde temperatures (Fig. 4) and Global Positioning System radio occultation (GPSRO) bending angles (30-36 km range, Fig.5). For radiosonde temperatures in the extra-tropics the bias is improved, whereas for GPSRO observations the bias is somewhat degraded. No other observations are currently assimilated or monitored to evaluate the cooling of the analysis around 1 hPa seen in Fig. 2 or the warming further above. Other independent observations such as retrievals from the Microwave Limb Sounder (MLS) or the Sounding of the Atmosphere using Broadband Radiometry (SABER) instrument tend to show mutual biases that exceed

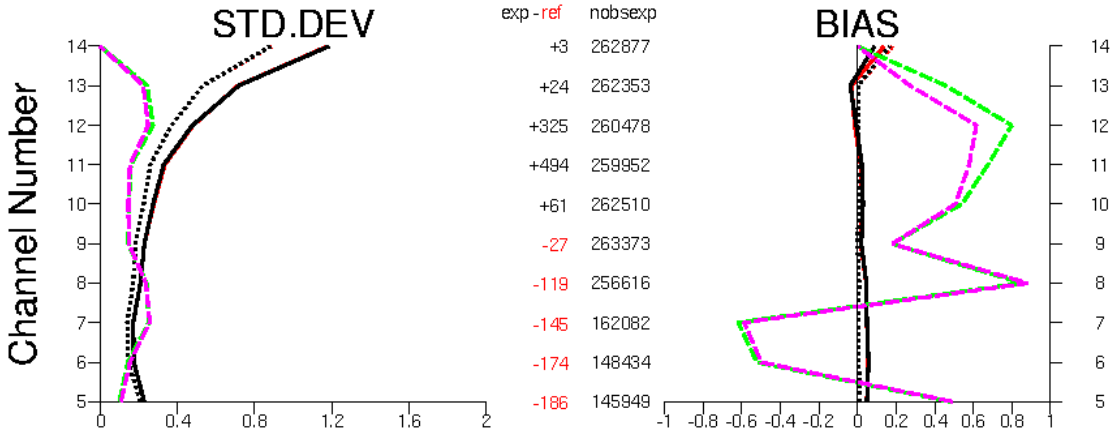

Figure 2: Standard deviations [K] (left panel) and means [K] (right panel) for FG departures (solid lines), analysis departures (dotted lines), and bias corrections (dashed lines) for used METOP-A AMSU-A radiances over the Southern Hemisphere for the period 16-30 September 2007 (observations minus FG or analysis, respectively). Statistics for the RT9 experiment are shown in black and magenta, whereas statistics for the Control experiment are shown in red and green. The number of used observations are displayed between the two plots, with the difference relative to the Control shown in the column "exp-ref".

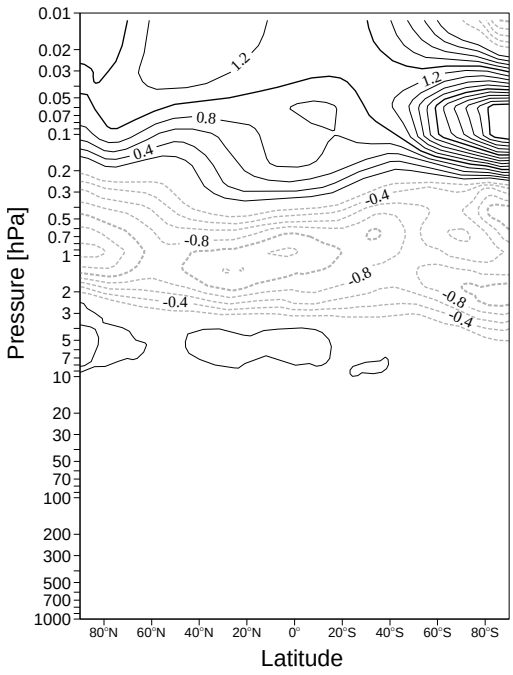

Figure 3: Zonal mean temperature difference [K] RT9 minus Control for the period 16-30 September 2007.

the differences shown here (Schwartz et al. 2008), rendering these data not useful to evaluate these relatively small differences.

Other differences in the mean bias corrections can be reported for the HIRS and AIRS water vapour channels, and for the AMSU-B/MHS humidity sounding channels. The differences are typically at most of the order of 0.3 K. For HIRS and AIRS, the bias correction for the water vapour channels are increased (in absolute terms), so an improvement is not immediately evident (e.g., compare red and black lines in Fig. 6c). Some changes

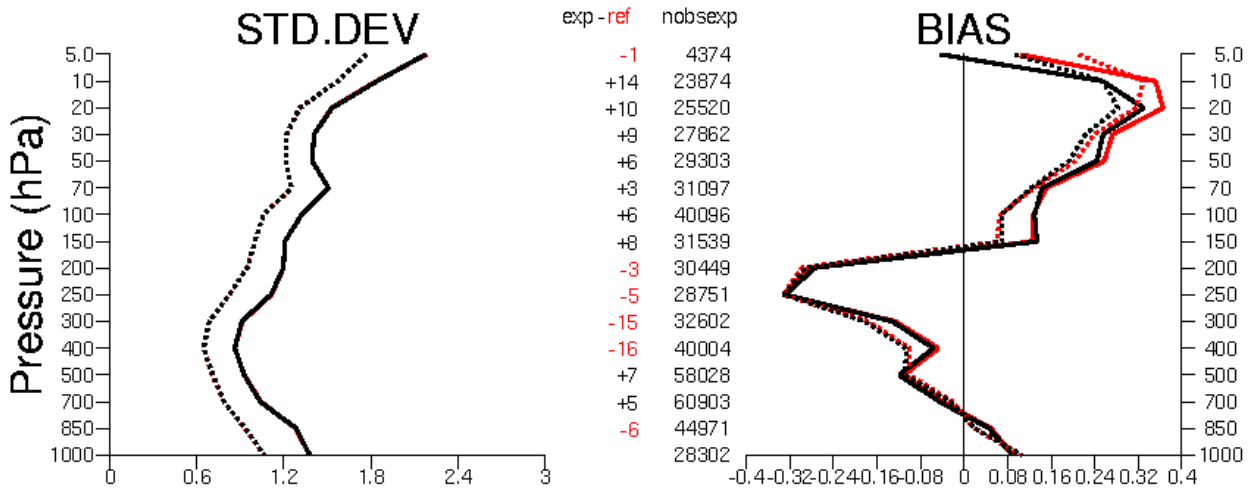

Figure 4: As Fig. 2, but for temperature observations from radiosondes as a function of pressure over the Northern Hemisphere.

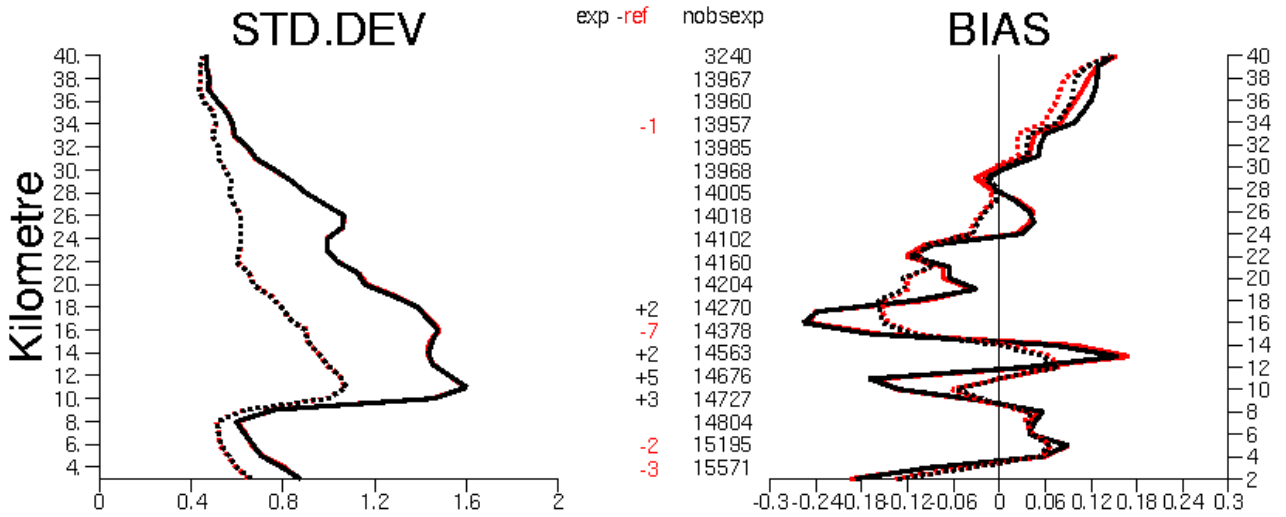

Figure 5: As Fig. 2, but for bending angles, normalised by the assumed observation error, from setting occultations of COSMIC-4 over the Northern Hemisphere.

in the bias correction can also be reported for AMSU-B/MHS (not shown). The responses in the water vapour channels are not accompanied with significant systematic adjustments in the mean humidity analysis.

After bias correction, FG or analysis departures for all radiances show little differences between the two experiments, in terms of mean departures, but also in terms of the standard deviations of the departures (e.g., Figures 2, 6a,b). This is not necessarily expected, as the improved radiative transfer modelling provided by RTTOV-9 should reduce the errors in the forward operator, therefore potentially leading to reductions in the standard deviations of the FG departures. However, it appears that a large proportion of the radiative transfer errors that have been altered through the two new features of RTTOV-9 used here are appearing as airmass-dependent biases. The effect of these has largely been taken into account empirically in the Control experiment through the bias correction.

Over the troposphere, departure statistics for other observations show little change between the experiments RT9 and the Control. Similarly, differences in the mean temperature or humidity analyses are small over the troposphere. Nevertheless, some more systematic differences can be reported for the geopotential above about 300 hPa, but again the differences are relatively small (e.g., Fig. 7).

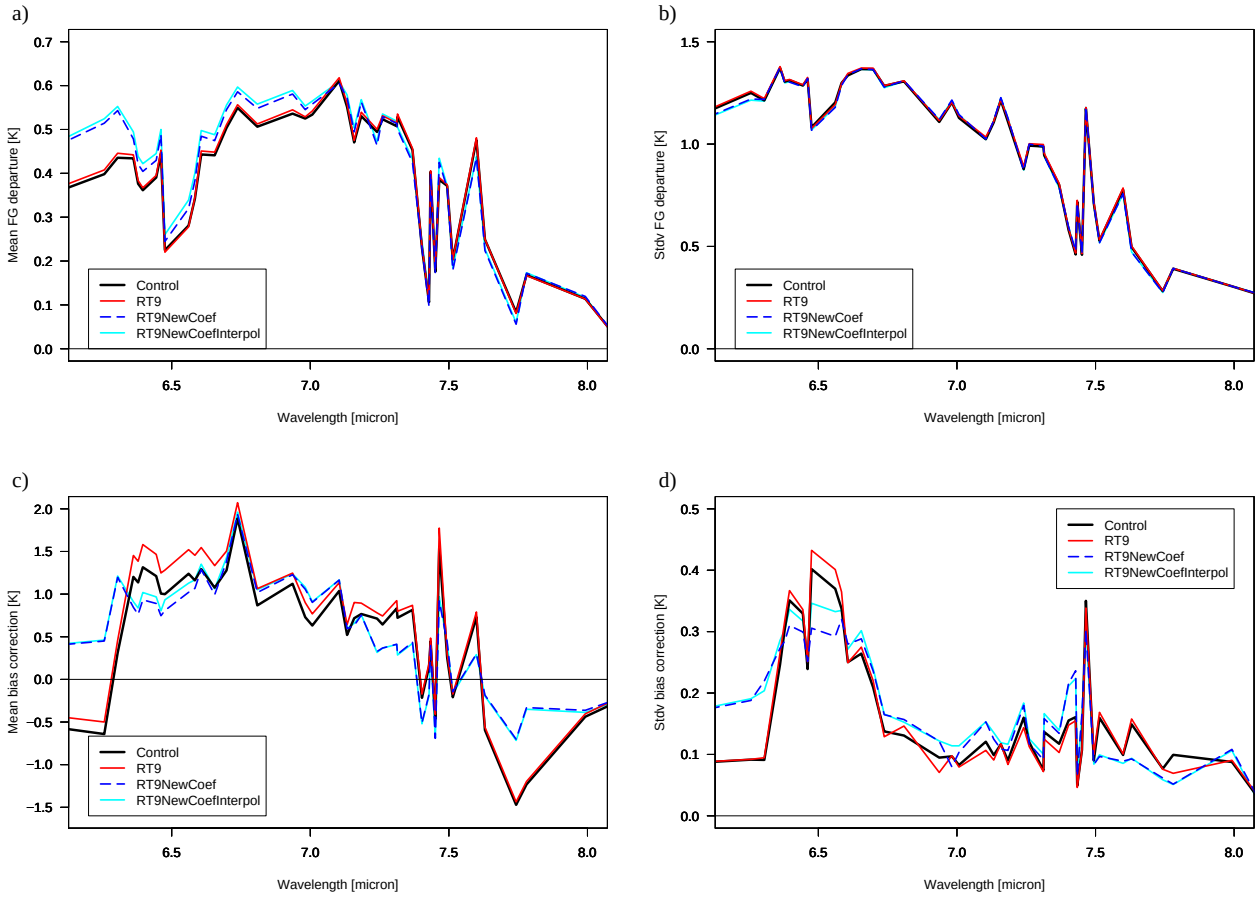

Figure 6: a) Mean FG departures (observations minus FG) for used AIRS channels in the water vapour band over the Northern Hemisphere for the period 16-30 September 2007 as a function of wavelength [µm] for the Control (black), RT9 (red), RT9NewCoef (dashed blue) and the RT9NewCoefInterpol (cyan) experiment. b) As a), but for the standard deviation of FG departures. c) As a), but for the mean bias correction. d) As a), but for the standard deviation of the bias correction.

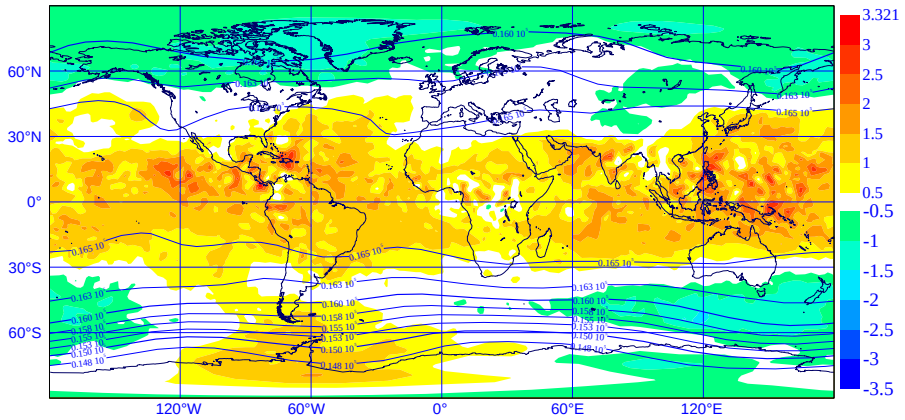

Figure 7: Shading indicates differences in the mean 100 hPa geopotential analysis [gpm] between the RT9 and the Control experiment (RT9-Control) over the period 16-30 September 2007. Contours display the mean 100 hPa geopotential [gpm] from the Control experiment.

3.3 New coefficient files

To characterise the effect of the new set of coefficient files we will now compare the experiments RT9 and RT9NewCoef.

Probably the largest difference for the coefficient file upgrade is the consistent use of kCARTA-derived radiative transfer coefficients with RTTOV-8 regression models. For the HIRS instruments, this leads to a substantial reduction (in absolute terms) in the mean bias corrections applied to all assimilated channels compared to the bias corrections necessary with the GENLN2-derived radiative transfer coefficients (Fig. 8). At the same time, standard deviations of FG departures and bias corrections are also slightly reduced for the lower tropospheric channels (6, 7, 14, 15) with the new coefficients. Given that tropospheric temperatures are rather well constrained in the assimilation system, the changes are viewed as a positive sign. They reflect a notable reduction in the forward model error and bias resulting primarily from the use of improved spectroscopy. The improvements in the temperature channels are primarily due to the inclusion of P/R-branch line mixing in kCARTA, whereas the improvements in the water vapour channels are due to updates in the HITRAN-database used in kCARTA. Similar substantial reductions in the absolute bias corrections are noticeable for the water vapour channels of the geostationary imagers (not shown).

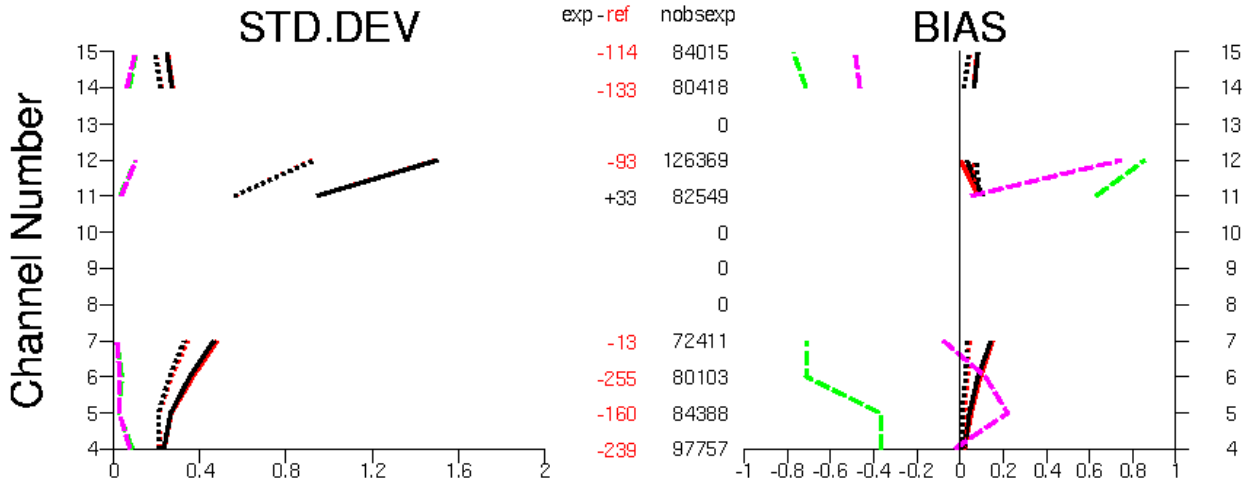

Figure 8: Standard deviations [K] (left panel) and means [K] (right panel) for FG departures (solid lines), analysis departures (dotted lines), and bias corrections (dashed lines) for used METOP-A HIRS radiances over the tropics for the period 16-30 September 2007 (observations minus FG or analysis, respectively). Statistics for the RT9NewCoef experiment are shown in black and magenta, whereas statistics for the RT9 experiment are shown in red and green. The number of used observations are displayed between the two plots, with the difference relative to RT9 shown in the column "exp-ref".

For the AIRS water vapour band, a reduction of the absolute bias corrections is also evident for a number of channels (compare red and blue lines in Fig. 6c), whereas FG departure statistics and standard deviations of bias corrections show comparatively small changes (other panels in Fig. 6). The smaller bias corrections are again a positive aspect, suggesting that the new coefficients reduce the bias in the radiative transfer simulations. Note, however, that for the GENLN2-derived coefficients used in RT9 the assimilated AIRS water vapour channels have non-unity γ-correction factors used for scaling the optical depths in the radiative transfer integration. These were derived empirically based on departure statistics from NWP. From our current experimentation it is therefore not possible to say whether the improvements are due to the use of kCARTA coefficients or the removal of the non-unity γs or both. Given that the γ factors were tuned using NWP, it is likely that the

reduction of the bias correction may be more dramatic if GENLN2 radiative transfer coefficients with unity γ factors had been used.

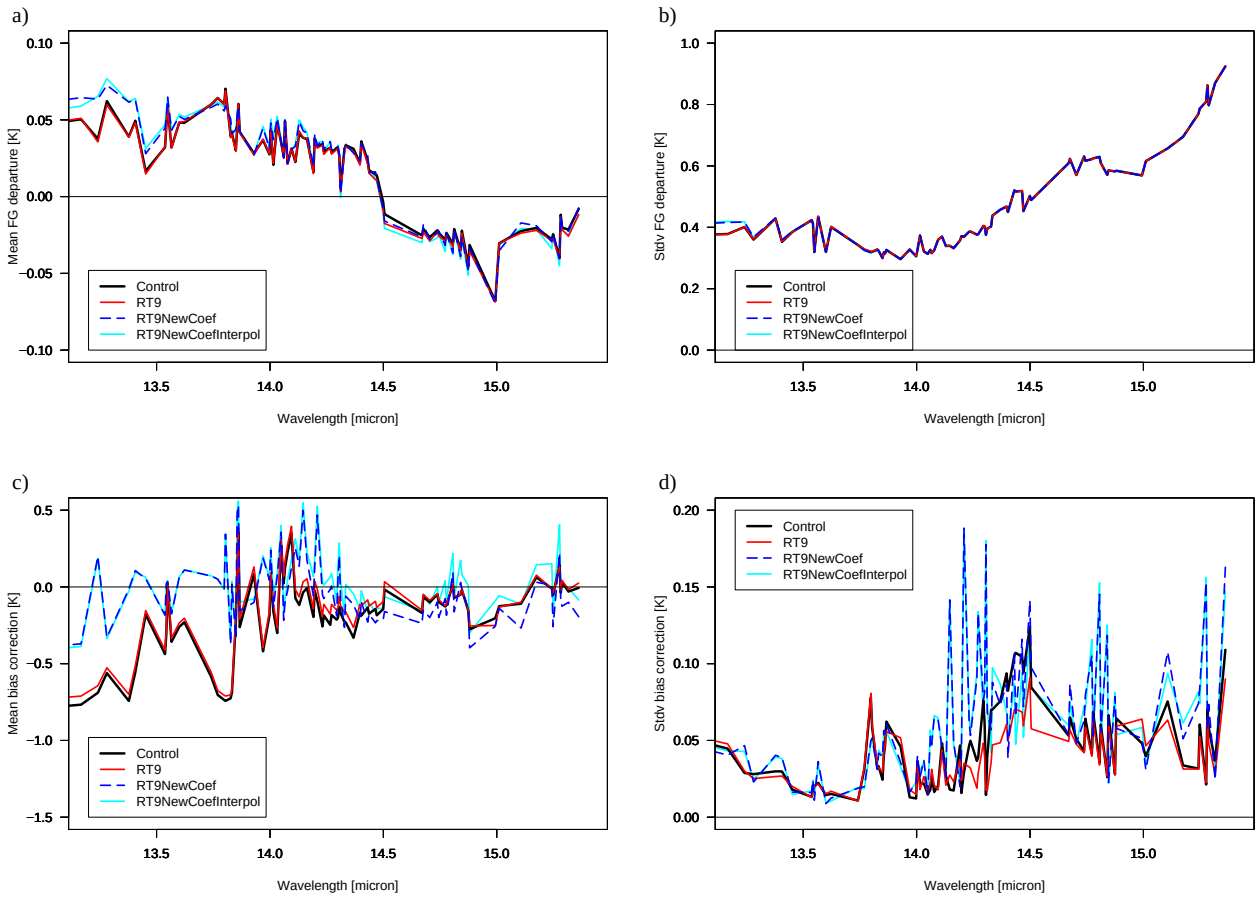

Figure 9: As Fig. 6, but for the 14 μm band for AIRS.

For the AIRS 14 μm band, the results are more mixed (Fig. 9). Below 14 μm, the use of kCARTA coefficients leads to a reduction of the absolute bias corrections, consistent with the findings for the HIRS instrument. Above 14 μm, some channels exhibit smaller absolute mean bias corrections, whereas others show increased bias corrections, especially around 14.15 μm. Above 14 μm, the standard deviation of the bias corrections is also considerably increased for some channels, suggesting that the bias correction model needs to represent more structure. This suggests that there is some benefit from using the GENLN2 coefficients or the NWP-based γ-coefficients in this spectral region.

For IASI, the move to the RTTOV-8 regression models instead of RTTOV-7 ones makes little difference in the 14 μm band (Fig. 10). Departure statistics and bias corrections appear more similar to the AIRS ones for the RT9NewCoef experiment.

The new RTTOV coefficient files for AMSU-B and MHS (more recent training set and use of FASTEM-3) and for AMSU-A or the microwave imagers (use of FASTEM-3) lead to only very minor differences to departure or bias correction statistics (not shown).

After bias correction, FG departure statistics for all radiances again do not show significant differences, except

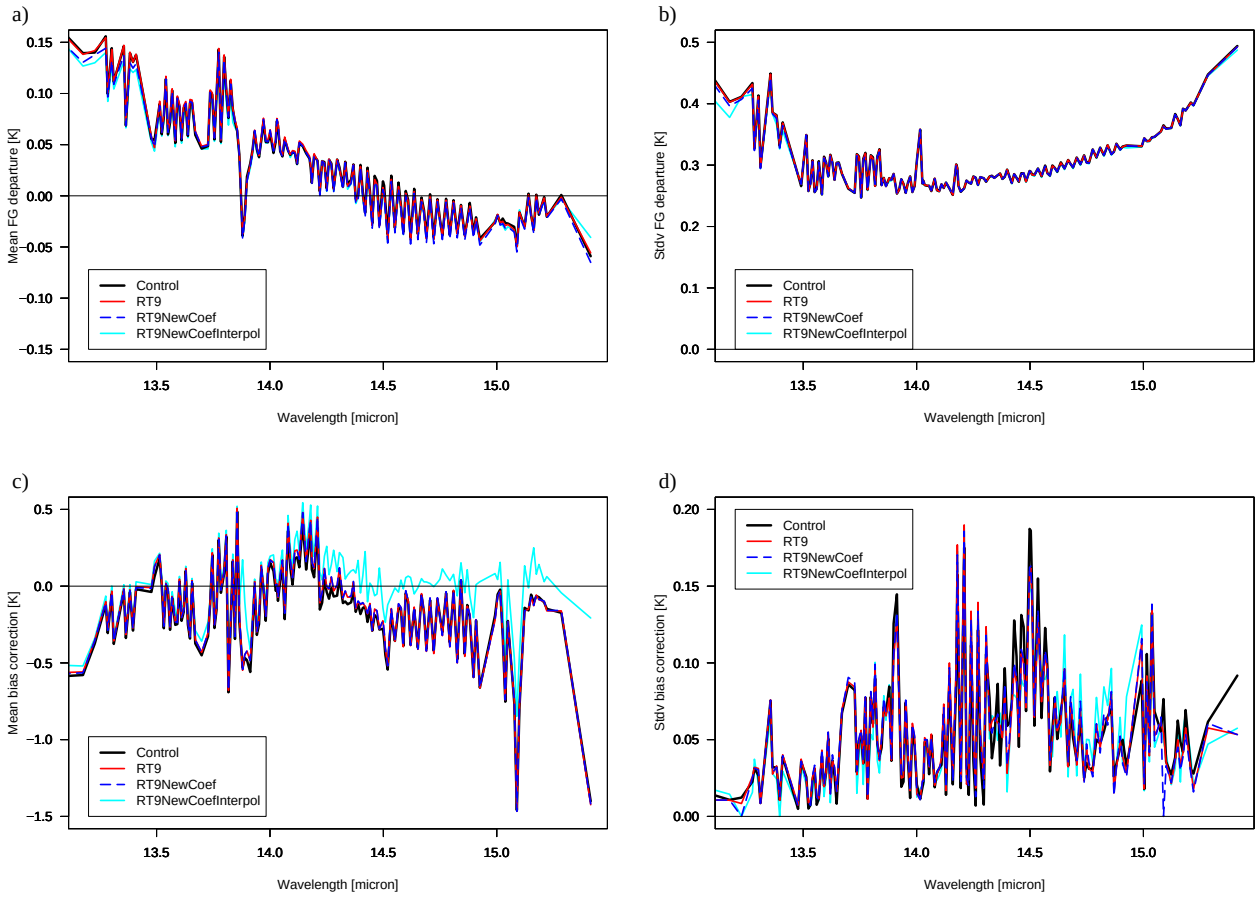

Figure 10: As Fig. 9, but for the used IASI channels.

for lower tropospheric HIRS channels (e.g., Figures 6, 8, 9, 10). This again suggests that the majority of the differences arising from the different radiative transfer coefficients are resulting in airmass-dependent biases, and the bias correction or adjustments in the mean model fields are able to respond to this. In this context it is worth pointing out that departure statistics for non-radiance observations show no significant differences between RT9 and RT9NewCoef, suggesting a similar quality of the FG and the analysis in the two experiments, at least as far as can be detected by the rest of the observing network.

Nevertheless, there are some systematic differences in the mean analyses, notably some temperature changes of a few tenth of a degree over the polar regions in the lower troposphere (Fig. 11), and small humidity changes. The changes are confined to regions without other unbiased temperature observations, so due to a lack of other observations it is impossible to evaluate whether these changes are an improvement or not.

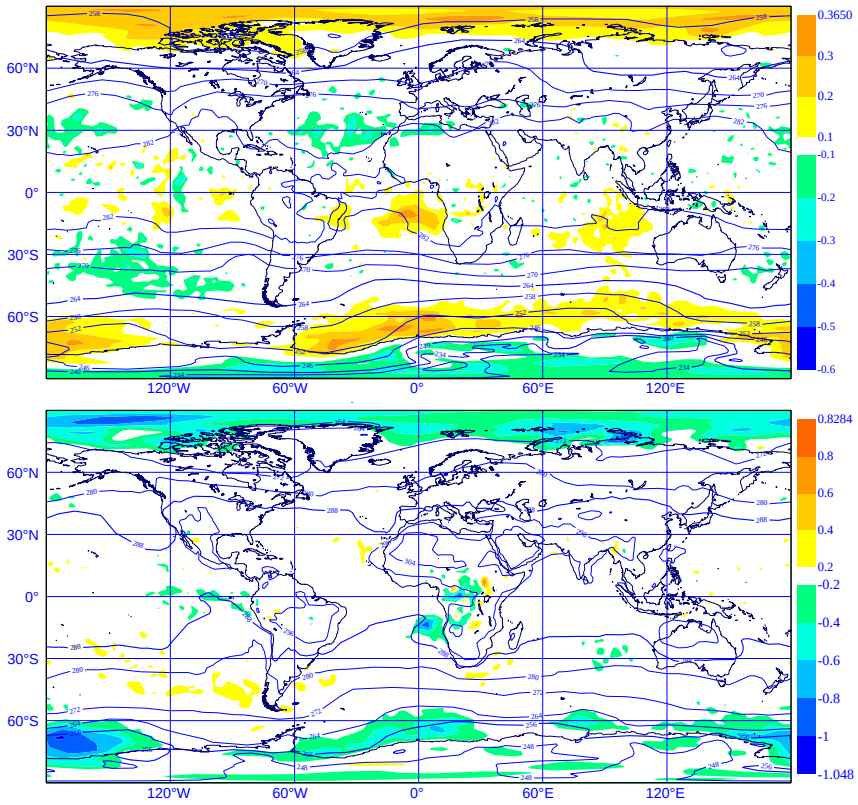

Figure 11: Shading shows the difference in the mean temperature analysis [K] at 700 hPa (top) and 925 hPa (bottom) between RT9NewCoef and RT9 over the period 16-30 September 2007. Red colours indicate a warming in RT9NewCoef. Contours display the mean temperature analysis of the Control.

3.4 Interpolation

We will now characterise the effect of activating the internal RTTOV-9 vertical interpolation instead of the linear interpolation used in the IFS. To do so, we compare experiments RT9NewCoefInterpol with RT9NewCoef. We recall here that the move to the RTTOV interpolation is not just a replacement of one interpolation method with another. Three aspects contribute (section 2.3): 1) the use of a smoother interpolator which leads to a different representation of the atmosphere for the optical depth calculations, 2) the use of the full IFS temperature profile to specify the source function in the radiative transfer integration, and 3) the reduced influence of RTTOV's unrealistic isothermal layer assumption near the top of the atmosphere, which implies that IFS information about the atmosphere above 0.1 hPa is ignored when the IFS interpolation is used. All three aspects are particularly important for the upper stratosphere/mesosphere where the RTTOV layering is relatively coarse (Fig. 1).

Arguably the most remarkable difference between experiments RT9NewCoefInterpol and RT9NewCoef are much improved gradients from the radiative transfer simulations, calculated for the minimisation of the data assimilation cost function (Fig. 12). While the use of the linear interpolation in the IFS leads to very noisy gradients with large unrealistic spikes, the internal RTTOV interpolation successfully retains the smooth structure of these gradients. This is a clear improvement, and is a result of the smoother nature of the interpolation.

The drastic change in the gradients on model levels from all radiance data has, however, relatively little impact on the overall size of the analysis increments as a result of the smoothing imposed by the background error correlations in the assimilation. This is highlighted in Fig. 13 which shows the global mean RMS of the

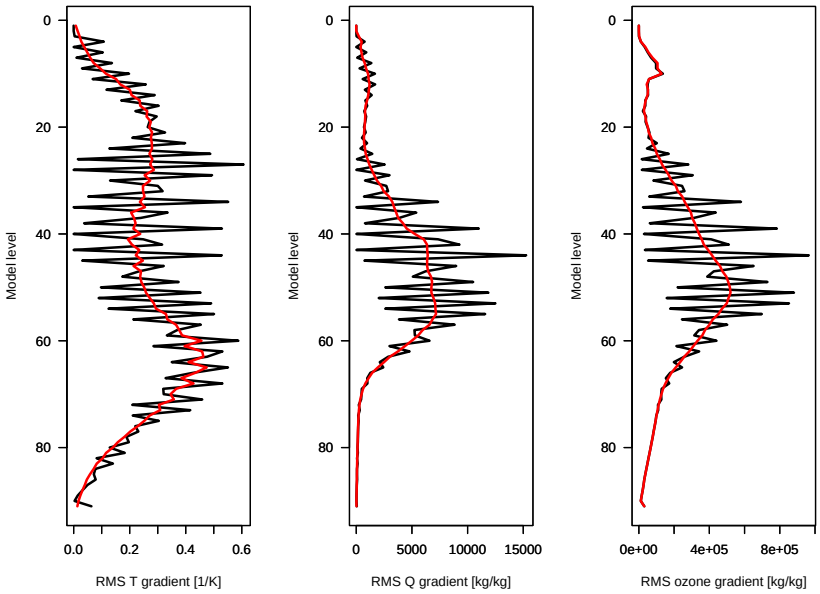

Figure 12: Root mean square of the initial temperature (left), humidity (middle), and ozone (right) gradients for all assimilated radiance observations for a single 12-hour assimilation cycle. Results with the IFS interpolation are shown in black, with the RTTOV internal interpolation in red.

temperature analysis increments. In the case of the IFS interpolation, the spikes seen in the gradients from the radiance observations are clearly not reflected in the analysis increments. The overall size of the increments at each model level is in fact similar in the two experiments at most levels, as the assumed background errors filter out any unrealistic small-scale structures. This does not mean that locally, the different gradients may not lead to meteorologicaly significantly different results. Also, it is clearly suboptimal to rely on the filtering effect of

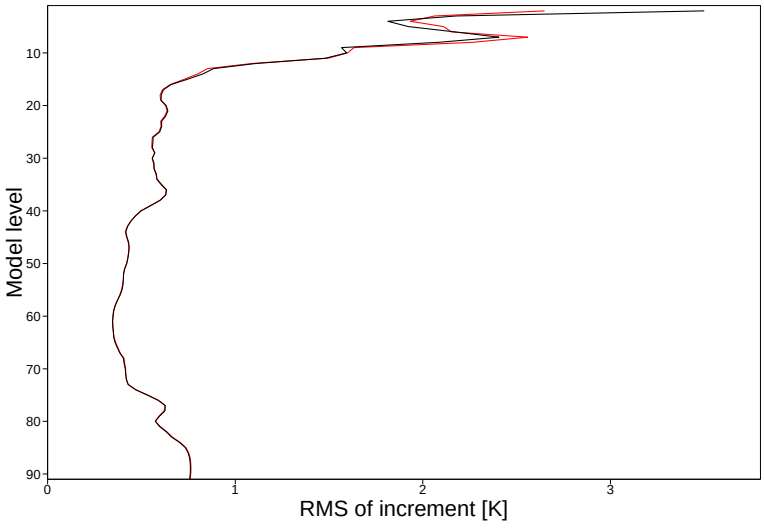

Figure 13: Global mean root mean square of the analysis increments in temperature [K] for the experiment which uses the IFS interpolation (black) and the one which uses the RTTOV interpolation (red) for the same assimilation cycle as shown in Fig. 12.

the background errors to correct unrealistic structures in the gradients produced by the observation operator.

Some difference in the general size of the increments exists towards the top of the model, above about model level 8 (0.5 hPa, Fig. 13). This is because the top two model levels were previously ignored in the radiance calculations when the IFS interpolation is used, as they lie above 0.1 hPa and are therefore affected by the RTTOV feature of an isothermal layer near the top of the atmosphere (section 2.3, see also Fig. 12 which shows a gradient of zero for the top levels when the IFS interpolation is used). The only constraint on these levels was previously through the background error correlations and the forecast model. In contrast, with the internal RTTOV interpolation these levels directly contribute to the radiance calculations, so the radiance assimilation provides a somewhat more direct (albeit still rather weak) constraint on them, the effect of which is also felt further below. Not surprisingly, this leads to a reduction in the overall size of the increments for the top two model levels, albeit at the expense of slightly larger increments for the levels directly below, followed by slightly smaller increments in the model level 11-25 range (1.7-28 hPa).

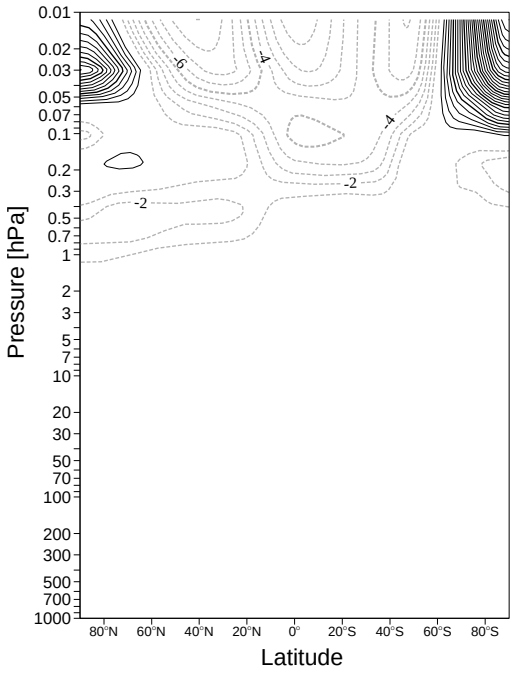

Figure 14: Difference in the zonal mean temperature analysis [K] between the experiment that uses the IFS interpolation and the one that employs the internal RTTOV interpolation. The contour interval is 1 K, and positive values, displayed in black solid, indicate warmer values when the RTTOV interpolation is used.

Also as a result of the improved handling of the top of the atmosphere in the experiment with the internal RTTOV interpolation, there are large differences in the mean temperature analyses for the top two model levels Fig. 14). Zonal mean differences exceed 20 K over the Southern Polar region, with more modest differences of less than 10 K over the tropics. This is again because radiance data put a somewhat more direct constraint on these levels when the internal RTTOV interpolation is used. The constraint imposed on these levels by the radiance assimilation is, however, relatively poor, as the weighting functions of all assimilated radiances peak well below the model top and the information on the top two levels therefore originates from the top tails of the weighting functions of few channels. Temperature retrievals from the Microwave Limb Sounder (MLS, Schwartz et al. 2008) have nevertheless been used to evaluate the changes in the temperature analyses towards the top of the atmospheric model, and this will be further discussed in section 4.2. The zonal mean bias changes are also a result of assimilating AMSU-A channel 14 without a bias correction, as the generally

different interpretation of the atmospheric profile information with the internal RTTOV interpolation will alter the bias characteristics for this channel which peaks around 2 hPa.

The differences near the model top also have significant effects on the bias corrections for some IASI channels in the 14 μm band, with high-peaking channels in the 14.4-15.5 μm range exhibiting the largest changes (Fig. 10). Further investigations reveal that the weighting functions for the most affected channels show relatively long tails towards the top of the model, with small, but non-zero contributions at the forecast model top (Collard, pers. communication). The RTTOV simulation for these channels are therefore more sensitive to RTTOV's assumption of an isothermal layer near the top of the atmosphere discussed in section 2.3. The effect of this assumption is reduced when the internal RTTOV interpolation is used, as temperature information from the IFS above 0.1 hPa is now used in the radiative transfer integration, with more realistic cooling with height above 0.1 hPa. As a consequence, the simulated FG equivalents now appear, overall, cooler, therefore leading to a reduction in the negative bias correction by several tenths of a Kelvin. It is encouraging that the analysis is now able to assimilate these IASI channels with bias corrections that are mostly closer to zero over the course of this experiment. The long-term interaction between the bias correction and the changes in the mean temperature analyses together with a general evaluation of the role of high-peaking channels in the assimilation deserves closer study in the future.

For the AIRS 14 μm band the situation is similar, although somewhat less pronounced in the sample of channels shown, as fewer high-peaking channels are assimilated than for IASI (Fig. 9). High-peaking AIRS channels that are passively monitored also show similarly sizeable changes in the mean bias correction (not shown). For the AIRS water vapour band, bias corrections show very similar characteristics with or without the external interpolation, except for a small increase in the mean bias correction and its standard deviation around 6.5 μm.

Other instruments also show some adjustments to the mean bias correction, resulting from the use of the internal RTTOV interpolation, but they tend to be fairly modest (at most 0.1 K), as they are less or not at all sensitive to the model top. For instance, most AMSU-A channels show a slight warming of the bias correction (Fig. 15). Due to the differences in the antenna pattern correction mentioned earlier, this means an increase in the bias

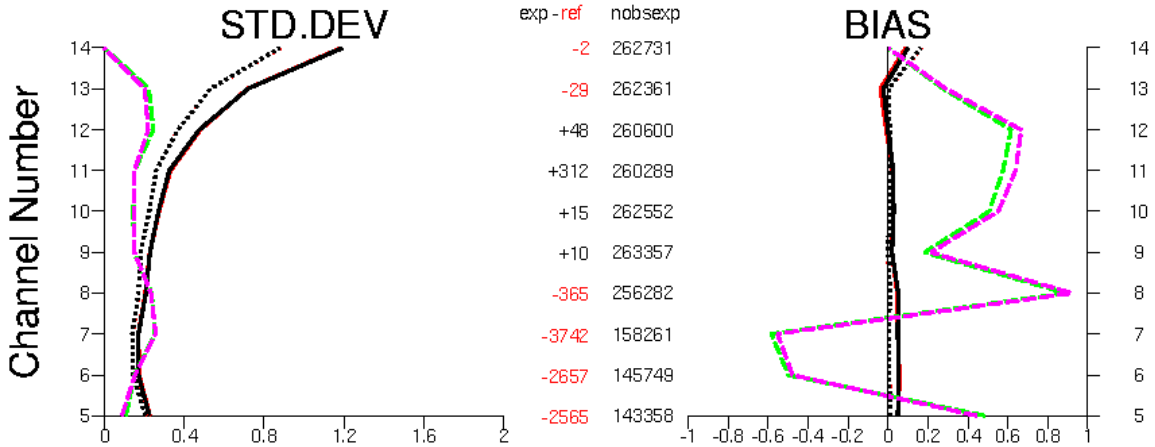

Figure 15: Standard deviations [K] (left panel) and means [K] (right panel) for FG departures (solid lines), analysis departures (dotted lines), and bias corrections (dashed lines) for used METOP-A AMSU-A radiances over the Southern Hemisphere for the period 16-30 September 2007 (observations minus FG or analysis, respectively). Statistics for the RT9NewCoefInterpol experiment are shown in black and magenta, whereas statistics for the RT9NewCoef experiment are shown in red and green. The number of used observations are displayed between the two plots, with the difference relative to the Control shown in the column "exp-ref".

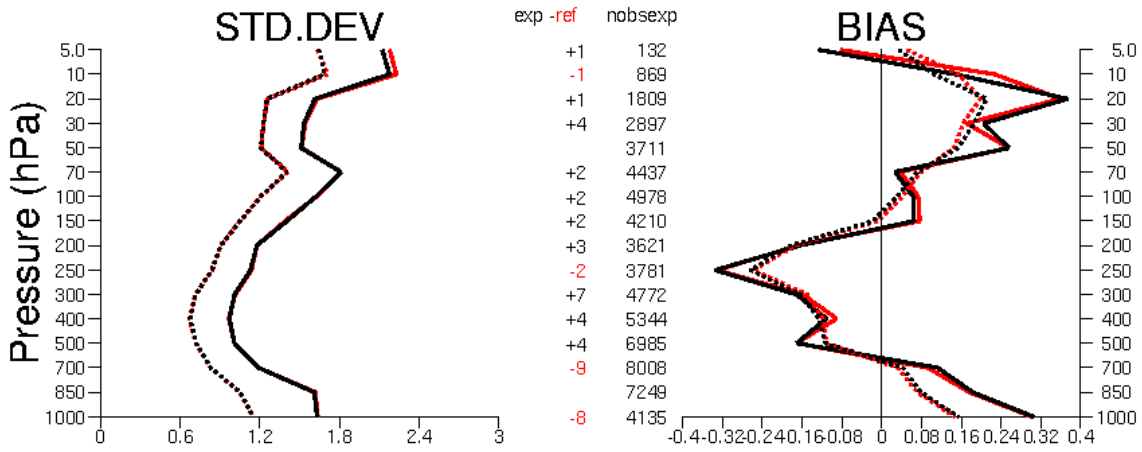

Figure 16: As Fig. 4, but for the experiments RT9NewCoefInterpol (black) and RT9NewCoef (red).

correction in absolute terms for the stratospheric AMSU-A channels of METOP, but a decrease for NOAA-18. Standard deviations of bias corrections are also reduced for channels 12 and 13, suggesting that the bias shows less structure. Similarly, the mid-tropospheric HIRS channels 4 and 5 and the water vapour channel 12 show a small warming in the mean bias correction (up to 0.1 K) which is an increase in the bias correction in absolute terms.

Other observations compare similarly well to the FG or the analyses in the experiments RT9NewCoefInterpol and RT9NewCoef. One noteworthy difference is a small change in terms of the bias in radiosonde temperature observations in the stratosphere (e.g., Fig. 16). The slight degradation around 30 hPa also appears as a change in the fit against GPSRO bending angles, where biases show an improvement for some satellites and a degradation for others. The improvement in the bias against the analysis at 5 and 10 hPa present in the radiosondes is not detected in the GPSRO data.

4 Analysis and forecast impact of the full upgrade

4.1 Experiments

The analysis and forecast impact of the full upgrade has been evaluated with extended experiments at higher resolution over two seasons. The experiments use the early delivery system of the IFS, with a 12-hour delayed cut off 4DVAR window. The model resolution is set at T511 (≈40 km), with an incremental analysis resolution of T159 (≈125 km), and 91 levels in the vertical. The control experiment uses the IFS version operational in autumn 2008 (35r1), whereas the RTTOV-9 experiment uses in addition the linear-in-tau parameterisation, the variable zenith angle, and the internal interpolation of RTTOV-9, and the updated set of coefficient files as described above. 10-day forecasts were run each day of the experiment from the 0 Z early-delivery analysis. The experiments cover, respectively the period 1 January to 5 March 2008, and 15 July to 15 September 2008. All experiments use a VarBC cold-start with the initial bias correction set to the mode of the FG departures, and we will discard the first 15 days of the experiments to allow VarBC to adjust to the bias conditions. Note that some spin-up for VarBC coefficients can occur after this period, for instance for some upper stratospheric temperature channels or humidity channels.

4.2 Analysis impact

The analysis impact and the characteristics of the assimilated radiances reflect a combination of the features described above for the individual contributions. For assimilated radiances the response is primarily via the bias correction. For the IR instruments, the changes in the bias correction statistics are largely dominated by the upgrade of the radiative transfer coefficient files as seen earlier (e.g., Fig. 8, 6, 9, and 10), and the statistics are not repeated here. For AMSU-A, the modifications to the bias correction statistics are a combination of the changes from the linear-in-tau parameterisation and the variable zenith angle and the use of the RTTOV internal interpolation, and as the changes had opposite signs, they combine to relatively little change when the control and the full RTTOV-9 upgrade are compared (not shown).

For the microwave instruments, AIRS, and the geostationary imagers, there is little change in the departure statistics after bias correction. HIRS shows a reduction in the standard deviations for the FG departure statistics for lower tropospheric channels noted earlier as a result of the move to the kCARTA-based radiative transfer coefficients (not shown).

In the January-March experiment, IASI exhibits a behaviour not observed in the earlier experiments: standard deviations of FG departures for high-peaking channels are reduced over the Northern Hemisphere for this experiment (Fig., 18), suggesting a better consistency of the system. Further investigations show that this reduction is a result of the use of the internal RTTOV-interpolation, and is mostly confined to an area between Scandinavia and Greenland. Relatively large changes in the mean bias correction for these channels were noted earlier as a result of the use of the internal RTTOV interpolation, and the related improved handling of temperature information from the top model levels. Maps of analysis increments also show reductions in the size of the increments associated with the north polar vortex throughout the stratosphere, further highlighting a better consistency of the system for this particular period (Fig. 19). A similar response is not observed on either hemisphere for the Northern Hemisphere summer experiment.

Zonal mean differences in the temperature analyses are shown in Figure 19 for the Northern Hemisphere winter experiment. These are dominated by the changes introduced through the RTTOV internal interpolation, and again mean changes of several K can be reported towards the top of the atmospheric model.

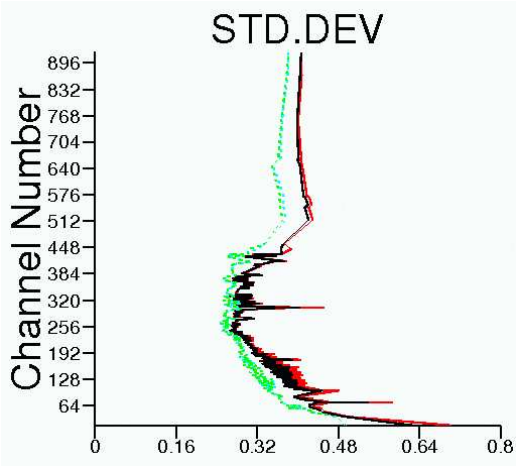

Figure 17: Standard deviations of departures [K] after bias correction for used IASI data over the Northern Hemisphere for the period 15 January 2008 to 15 February 2008. Statistics for FG departures for the control experiment are shown in red, and those for the RTTOV-9 experiment are shown in black. Statistics for the analysis departures are shown in green for the control and in cyan for the RTTOV-9 experiment.

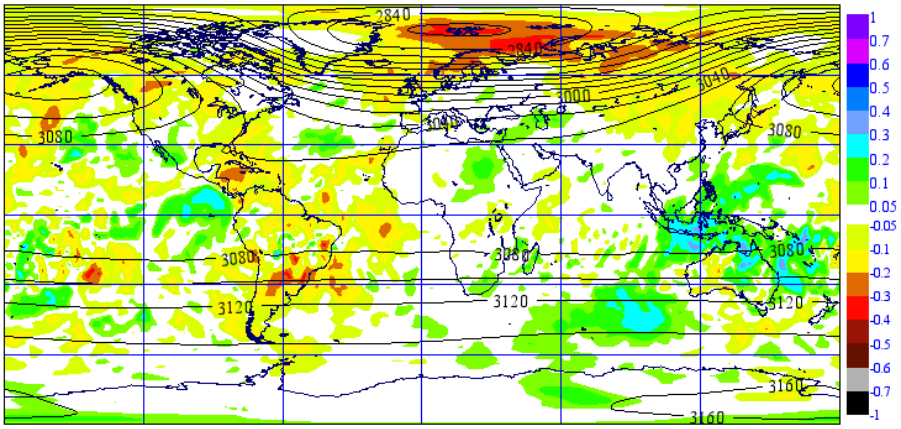

Figure 18: Shading shows normalised differences in the root mean square of the analysis increments for the 10 hPa geopotential for the period 15 January - 15 February 2008 between the RTTOV-9 experiment and the Control. Yellow/red/brown colours indicate reduced increments for the RTTOV-9 experiment. Contours show the mean 10 hPa geopotential [gpdm] for the Control experiment.

It is largely futile to evaluate the temperature changes near the top of the forecast model given the poor representation of these layers in the model, the poor constraint of the analysis on these layers, and the limitations of temperature observations available for evaluation of these levels. Nevertheless, the changes observed in these experiments have been evaluated with temperature retrievals from the Microwave Limb Sounder (MLS) onboard the Aura satellite. The instrument uses limb emissions to provide information on atmospheric temperature and trace gas profiles. The vertical resolution of the temperature profiles is around 3.5 km at 31.6 hPa,

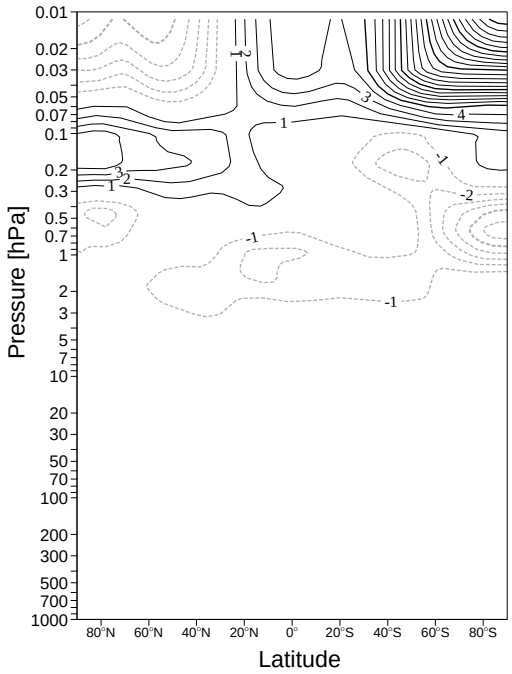

Figure 19: Difference in the zonal mean temperature analysis [K] between the RTTOV-9 experiment and the control for the period 15 January - 5 March 2008. The contour interval is 1 K, and positive values, displayed in black solid, indicate warmer values in the RTTOV-9 experiment.

dropping to 6.2 km at 3.16 hPa and ≈14 km at 0.01 hPa. The theoretical precision of the temperature retrievals is 1 K or better below 0.316 hPa, and increases to around 2.2 K at 0.01 hPa. MLS profiles have been compared against other retrievals and model data (Schwartz et al. 2008). From 316 hPa to ≈10 hPa there is generally good agreement to within ≈1.5 K compared to ECMWF analyses, radiosondes, AIRS or CHAMP retrievals. Further above, MLS exhibits biases with respect to SABER retrievals of a few Kelvin. In the troposphere and lower stratosphere, MLS tends to exhibit vertical oscillations compared to other temperature data, with an amplitude of 2-3 K and a vertical frequency of about 1.5 cycles per decade of pressure.

The experiments have been compared to MLS retrievals for a 10-day period each, covering 1-10 February 2008, and 21-31 August 2008, respectively. To do so, analyses have been spatially interpolated to the locations of the MLS retrievals, and both have been interpolated vertically to a common grid. The results from these comparisons are somewhat mixed. They show that the Control and the RTTOV-9 experiments have a broader and occasionally higher stratopause than MLS for most regions (e.g., Fig. 20a), leading to a lower mesosphere that tends to be warmer than suggested by MLS, typically by up to 5-20 K (e.g., Fig. 20b). The exception is the South Polar region which will be discussed further below. The RTTOV-9 upgrade does little to the sharpness of the stratopause (e.g., Fig. 20a), as expected, as little additional information on the vertical structure is provided. For the Northern Hemisphere summer experiment, there is a tendency for the RTTOV-9 upgrade to decrease the warm bias versus MLS over most regions, whereas results are mixed for the Northern Hemisphere winter experiment. For both experiments, the RTTOV-9 experiment appears to capture the general spatial temperature structure in better agreement with MLS for some regions, as evidenced by smaller standard deviations of the differences (e.g., Fig. 20b for the North Polar region and the Northern Hemisphere winter experiment). For the South Polar region, the results are somewhat different: here, the Control experiment for the Northern Hemisphere winter shows a stratopause in very good agreement with MLS, and the RTTOV-9 upgrade degrades this by lowering the stratopause and warming the mesosphere in the top model levels (Fig. 20c). In contrast, the Northern Hemisphere summer experiment shows a sharper stratopause than MLS in both IFS experiments (Fig. 20d), leading to a colder mesosphere in the model fields compared to MLS. The latter is considerably reduced in the RTTOV-9 experiment, bringing the analyses in closer agreement to MLS. In summary, we conclude that despite a slight advantage for the RTTOV-9 experiments neither the Control nor the RTTOV-9 experiments clearly perform better compared to MLS data near the model top, despite the drastic changes to the mean temperature analyses, and quite considerable deviations against MLS data near the forecast model top exist in both experiments.

4.3 Forecast impact

The forecast impact from the RTTOV-9 upgrade over the two periods investigated is neutral. Mean tropospheric forecast scores for geopotential, wind, and relative humidity are, overall, not statistically significantly different for the RTTOV-9 experiments and the Control (Figures 21, 22). This, to some extent reflects the relatively neutral changes in terms of the FG departure statistics after bias correction noted throughout this memorandum for the radiances. Some forecast improvements from the RTTOV-9 upgrade are present in the short range for the stratospheric north polar vortex for the January-March experiment, consistent with the reduced increments noted earlier (not shown); yet these improvements do not carry on beyond day 2.

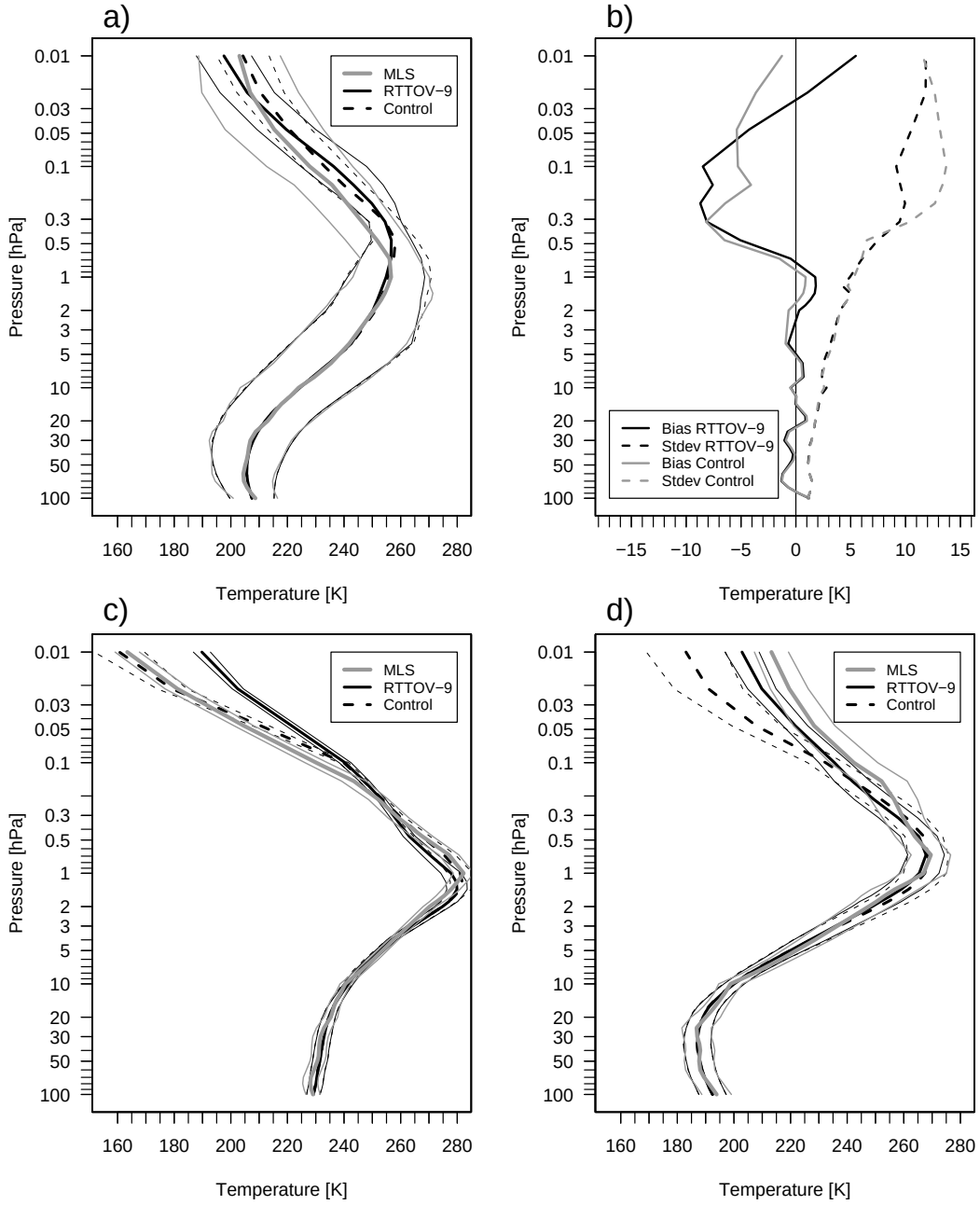

Figure 20: a) Mean temperature profiles (thick lines) over the North Polar region (north of 60N) and the period 1-10 February 2008 for the MLS retrievals (grey), the RTTOV-9 experiment (black solid), and the control (black dashed). Thin lines indicate one standard deviations from the mean profile. Statistics are based on 5624 MLS profiles. b) Bias (MLS minus analysis, solid lines) and standard deviations (dashed) of the differences between MLS temperature retrievals and the analyses for the RTTOV-9 experiment (black) and the control (grey). Statistics have been calculated for the North Polar region (north of 60N) and the period 1-10 February 2008 and are based on 5624 MLS profiles. c) As a), but for the South Polar region (south of 60S), based on 5665 MLS profiles. d) As c), but for the period 21-31 August 2008, based on 6178 MLS profiles.

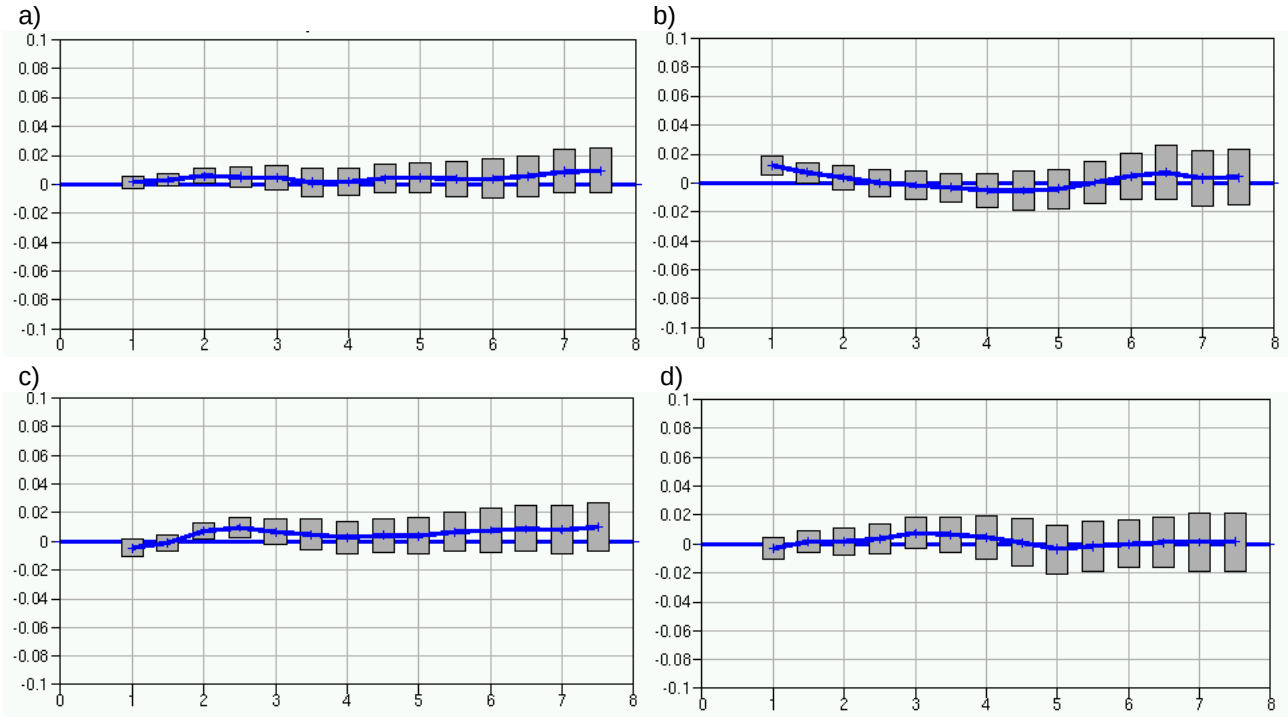

Figure 21: a) Normalised differences in the root mean square forecast error for the 500 hPa geopotential over the Northern Hemisphere between the RTTOV-9 experiments and the Control as a function of forecast range in days (97 cases). Both experiments have been verified against the operational ECMWF analysis. Negative values indicate a reduction in forecast error for the RTTOV-9 experiment. Error bars indicate confidence intervals at the 90 % confidence level. b) As a), but for the Southern Hemisphere. c) As a), but for the 200 hPa geopotential. d) As b), but for the 200 hPa geopotential.

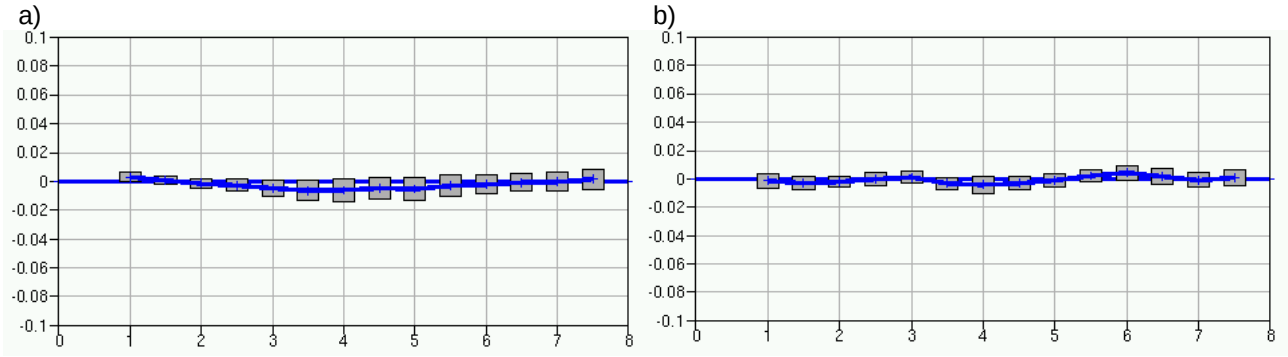

Figure 22: a) Normalised differences in the root mean square forecast error for the 850 hPa wind over the tropics between the RTTOV-9 experiments and the Control as a function of forecast range in days (97 cases). Both experiments have been verified against the operational ECMWF analysis. Negative values indicate a reduction in forecast error for the RTTOV-9 experiment. Error bars indicate confidence intervals at the 90 % confidence level. b) As a), but for the 100 hPa wind.

5 Conclusions

This memorandum summarises the impact of the upgrade to RTTOV-9 on analyses and forecasts in the ECMWF system. The upgrade included the activation of the linear-in-tau parameterisation of the layer source function, the use of a variable zenith angle, the use of the internal RTTOV-9 interpolation in the vertical, and a revision of the set of radiative transfer coefficient files. The main findings are:

- The upgrade affects particularly the bias correction characteristics for the assimilated radiances. One of the largest changes is due to the move to kCARTA-based RTTOV coefficients which leads to a significant reduction of the absolute size of the corrections for HIRS. Use of the internal interpolation, and application of the other new RTTOV-9 features also contribute to changes in the required bias correction.
- After bias correction, most departure statistics for assimilated radiances are overall largely unaltered. Exceptions are reductions in the size of FG departures for lower tropospheric HIRS channels resulting from the kCARTA coefficients, and, for specific periods, reductions in the size of some high-peaking IASI channels which benefit from improvements related to the use of the RTTOV internal interpolation.
- The use of the RTTOV internal interpolation successfully avoids spikes previously seen in gradients from the radiance data on model profiles. However, globally, this has little influence on the size of increments for a given model level.
- Enabling the RTTOV internal interpolation leads to an improved use of FG temperature information near the model top, resulting in significantly different bias corrections and occasionally reduced FG departures for some high-peaking IASI channels. Use of the internal interpolation means that temperature information above 0.1 hPa is now used in the radiative transfer calculations, whereas previously it was ignored. This also leads to considerable differences in the mean temperature analysis near the forecast model's top.
- The forecast impact over the troposphere over the two periods considered is overall neutral.

The finding that FG departure statistics after bias correction are largely unaltered for most channels stresses the importance of the bias correction and the bias models for the radiance assimilation. It suggests that the improvements in the radiative transfer modelling included in this upgrade largely address air-mass dependent biases, and these appear to project well onto the current bias correction models. In turn, this emphasises the need for the chosen bias model to be able to reflect the characteristics of such air-mass dependent biases, in order for the detection of such biases due to the radiative transfer to be most successful. Detection of the biases by the variational bias correction will work best in areas for which the analysis is well-anchored by other observations.

Some of the largest improvements beyond what can be compensated for through the bias correction were found for the upgrade to kCARTA-based coefficient files for the infrared instruments. This highlights the importance of the training data underlying the RTTOV coefficients, and emphasises the need to keep the set of coefficient files used in the assimilation up-to-date. Note that updating coefficient files is technically much easier than upgrading the RTTOV software (the update of the set of coefficient files studied here could have been performed without RTTOV-9). New coefficient files based on LBLRTM calculations have recently become available for infrared sensors (e.g., Matricardi and McNally 2008), and their benefits in an assimilation context should be studied.

Some of the more surprising improvements in terms of size of the bias corrections and FG departures are related to the handling of FG information near the model top. Some high-peaking IASI channels assimilated

appear to have sufficient sensitivity to the top-most model levels to benefit from improvements in this area. Effects of this can locally be felt considerably further below, down to about 50 hPa. Note that despite the improvements introduced here, RTTOV-9 still handles the top layer sub-optimally: for instance, it ignores temperature, humidity, and ozone profile information above 0.1 hPa for the optical depth calculations, and instead uses the values given for 0.1 hPa for the highest radiative transfer layer. The experience here suggests that the high-peaking IASI channels would benefit from a proper handling of the top layer in RTTOV, as planned for RTTOV-10. The use of the high-peaking channels, their radiative transfer modelling, and the role of the model representation near the top deserve some further investigations.

Acknowledgements

RTTOV is developed through the EUMETSAT NWP SAF. The development efforts are coordinated by Roger Saunder's (Met.Office). Pascal Brunel (Météo France) provided the kCARTA coefficient files used in this study. Discussions with Carole Peubey and Andrew Collard regarding RTTOV-9 monitoring statistics are gratefully acknowledged.

References

Deblonde, G., and S. English, 2001: Evaluation of the fastem-2 fast microwave oceanic surface emissivity model. In Tech. Proc. ITSC-XI Budapest, 67–78.

Dee, D., 2004: Variational bias correction of radiance data in the ECMWF system. In ECMWF Workshop on Assimilation of High Spectral Resolution Sounders in NWP, ECMWF, Reading, UK, 97–112.

DeSouza-Machado, S., L. Strow, and S. Hannon, 1997: kcompressed radiative transfer algorithm (kcarta). In In Proceedings of the European Aerospace Remote Sensing #3220, Institute of Electrical Engineers, London, Great Britain.

DeSouza-Machado, S., L. Strow, and S. Hannon, 1999: Improved atmospheric radiance calculations using co_2 p/r branch line mixing. In In Proceedings of the European Aerospace Remote Sensing #3867, Florence, Italy.

Edwards, D., 1992: GENLN2: A general line-by-line atmospheric transmittance and radiance model. Technical note TN-367+STR, NCAR, Boulder, CO, USA.

Geer, A., P. Bauer, and P. Lopez, 2008: Lessons learnt from the operational 1D + 4D-Var assimilation of rain- and cloud-affected SSM/I observations at ECMWF. *Quart. J. Roy. Meteor. Soc.*, **134**, 1513–1525.

Kobayashi, S., M. Matricardi, D. Dee, A. McNally, and S. Uppala, 2007: Recalculation of rttov coefficients for amsu-a. Research Department Memorandum 0763, ECMWF, Reading, UK.

Liebe, H., 1989: Mpm - an atmospheric millimetre-wave propagation model. *Int.J.Infrared Milli.*, **10**, 631–650.

Liebe, H., P. Rosenkranz, and G. Hufford, 1992: Atmospheric 60-ghz oxygen spectrum: new laboratory measurements and line parameters. *J.Quant.Spectrosc.Radiat.Transfer*, **48**, 629–643.

Matricardi, M., 2003: RTIASI-4, a new version of the ECMWF fast radiative transfer model for the infrared atmospheric sounding interferometer. Technical Memorandum 425, ECMWF, Reading, U.K., 63 pp [available under www.ecmwf.int/publications/library/do/references/list/14].

Matricardi, M., 2005: The inclusion of aerosols and clouds in rtiasi, the ecmwf fast radiative transfer model for the infrared atmospheric sounding interferometer. Technical Memorandum 474, ECMWF, [available from http://www.ecmwf.int/publications/library/references/list/14].

Matricardi, M., F. Chevallier, and J.-N. Thépaut, 2004: An improved general fast radiative transfer model for the assimilation of radiance observations. *Quart. J. Roy. Meteor. Soc.*, **130**, 153–173.

Matricardi, M., F. Chevallier, and S. Tjemkes, 2001: An improved general fast radiative transfer model for the assimilation of radiance observations. Technical Memorandum 345, ECMWF, Reading, U.K., 40 pp [available under www.ecmwf.int/publications/library/do/references/list/14].

Matricardi, M., and A. McNally, 2008: An assessment of the accuracy of the rttov fast radiative transfer model using iasi data. In Proceedings of the 16th international TOVS study conference, Angra dos Reis, Brazil, CIMSS, University of Wisonsin, Madison, US, in press.

Rochon, Y., L. Garand, D. Turner, and S. Polavarapu, 2007: Jacobian mapping between vertical co-ordinate systems in data assimilation. *Quart. J. Roy. Meteor. Soc.*, **133**, 1547–1558.

Saunders, R., M. Matricardi, and P. Brunel, 1999: An improved fast radiative transfer model for assimilation of satellite radiance observations. *Quart. J. Roy. Meteor. Soc.*, **125**, 1407–1426.

Saunders, R., M. Matricardi, and A. Geer, 2008: Rttov9.1 users guide. Nwp saf report, Met.Office, 57pp.

Schwartz, M., A. Lambert, G. Manney, W. Read, N. Livesey, L. Froidevaux, C. Ao, P. Bernath, C. Boone, R. Cofield, W. Daffer, B. Drouin, E. Fetzer, R. Fuller, R. Jarnot, J. Jiang, Y. Jiang, B. Knosp, K. Krüger, J.-L. Li, M. Mlynczak, S. Pawson, J. Russell III, M. Santee, W. Snyder, P. Stek, R. Thurstans, A. Tompkins, P. Wagner, K. Walker, J. Waters, and D. Wu, 2008: Validation of the aura microwave limb sounder temperature and geopotential height measurements. *J. Geophys. Res.*, **113**, D15S11, doi:10.1029/2007JD008783.

Sherlock, V., 1999: Isem-6: Infrared surface emissivity model for rttov-6. NWP SAF report, Met.Office.

Watts, P., and A. McNally, 2004: Identification and correction of radiative transfer modelling errors for atmospheric sounders: AIRS and AMSU-A. In ECMWF Workshop on Assimilation of High Spectral Resolution Sounders in NWP, ECMWF, Reading, UK, 23–38.